Available online at www.sciencedirect.com

ScienceDirect

Current Opinion in Electrochemistry

Review Article

Structural transformations of metal alloys under electrocatalytic conditions

Yunfei Wang[1], Tianyao Gong[1], Matthew Lee[1] and Anthony Shoji Hall[1,2]

Abstract

Nanostructured alloys are efficient catalysts for mediating renewable energy storage and recovery reactions. The morphology and composition of an alloy can change during catalysis; particularly for potentials more oxidizing than the reversible hydrogen electrode. The formation of noble-metal shells covering an alloy core, or bi-continuous nanoporosity, is a common way an alloy can evolve by a corrosion mediated process. Recently, it was found that alloys can reconstruct within the bulk and form an ordered intermetallic material with different crystal structures and compositions than the starting material during corrosion. This review will discuss the different pathways alloys can be altered by electrochemistry. We will discuss the mechanisms which cover known structural changes and the more recently discovered process involving electrochemically driven incongruent phase transformations. Insights into the transformation of alloy materials are important for understanding how to prepare catalysts with improved electrochemical stability, and for synthesizing materials.

Addresses

[1] Department of Materials Science and Engineering, Johns Hopkins University, Baltimore, MD 21218, USA

[2] Department of Chemistry, Johns Hopkins University, Baltimore, MD 21218, USA

Corresponding author: Hall, Anthony Shoji (shoji@jhu.edu)

Current Opinion in Electrochemistry 2021, **30**:100796

This review comes from a themed issue on **Innovative Methods in electrochemistry (2021)**

Edited by **Plamen Atanassov** and **Wolfgang Schuhmann**

For complete overview about the section, refer Innovative Methods in electrochemistry (2021)

Available online 7 July 2021

https://doi.org/10.1016/j.coelec.2021.100796

Keywords

Dealloying, Phase transformations, Alloys, oxygen reduction reaction, ORR, Phase transformation, Core-shell, Ordered intermetallic catalyst, Ordered intermetallic, Stability, Durability, Nanomaterial, Electrocatalysis, Electrochemistry.

Introduction

Electrocatalysts play an important role in the development of sustainable energy technology because it is a critical component for fuel cells [1], water electrolysis [2,3], and the electrosynthesis of molecules to value-added products [4,5]. In the last two decades, advancements in the fundamental knowledge of chemical catalysis and the preparation of nanomaterials have led to improvements in electrochemical performance [6]. However, maintaining the stability of nanostructured materials during electrocatalysis is a critical challenge because nanomaterials are inherently thermodynamically unstable [7]. Improved stability for nanostructured alloys under electrochemical conditions is important for the commercialization of renewable-energy—based electrochemical devices for several reasons, such as (i) commercial electrochemical devices require stability to be reliable for maintaining performance over a long period of time [8] (ii) structural changes can make it difficult to correlate catalyst activity to structure, and (iii) the corrosion of the catalyst can cause contamination to other components in the device, reducing efficiency [9,10].

One of the primary modes of instability for nanostructured alloys is the oxidation and dissolution of the non-noble metal component. This manuscript will focus on recent developments in the morphological and structural evolution of complex nanomaterials when subject to oxidizing voltages in aqueous solutions. We will begin this review by introducing some of the conventional wisdom regarding binary alloy transformations under oxidizing conditions. Next, we will discuss electrochemically driven incongruent phase transformations of ordered intermetallic materials. Insights into the structural evolution of materials under electrochemical conditions are critical for understanding the dynamic changes of catalyst active sites and for developing new ways of synthesizing materials.

Structural evolution of multi-metallic nanomaterials

Nanomaterials can undergo structural, compositional, and morphological changes during electrochemical catalysis. Modifications to the catalyst are commonly observed during the oxygen reduction reaction (ORR) because the potential limit, between ~0.6 and 1.0 V versus the reversible hydrogen electrode, is oxidizing to most elements. Consequently, understanding material stability under ORR operating conditions has been a major focus of research.

Early reports of improved ORR electrocatalysis on Pt alloyed with transition metals such as Ti, V, Mn, Mo, and Al were from patents awarded to United Technologies (International Fuel Cells) in the 1980s [11–15]. It was found that alloys with a composition of Pt_xM_{1-x} (x = 0.6 to 0.75) lost up to ~35% or ~70% of the non-noble metal component when M was Cr or V, respectively, during ORR stability testing. Besides this information, little was known about the structure of the material until more rigorous investigations of catalyst stability were performed in the early 1990s on the Pt_3Co system by Beard and Ross [16]. It was found that the Pt_3Co alloy lost ~15% of the Co during ORR testing. In 1994, Watanabe et al. [17] proposed that the non-noble element corroded from the surface of Pt_3Co alloys; they suggested that a Pt-skin formed over the alloy core. Later, a report by Watanabe et al. [17] in 1999 found that pure Pt skins were formed on Pt-M (M = Ni, Co, Fe) alloys for various compositions as probed by X-ray photoelectron spectroscopy [18]. Several studies have found that the performance and stability of the Pt-skin layer can be substantially altered by its method of formation. There are three dominant pre-treatment strategies, chemical dealloying, high-temperature annealing, or electrochemical dealloying; the latter two methods typically result in the formation of Pt skins [19–24]. High-temperature annealing is valuable for the preparation of Pt skins on bulk electrodes, but this method can cause a decrease in the surface area and alter the morphology of nanoparticles, which may be unfavorable or beneficial depending on the application

Figure 1

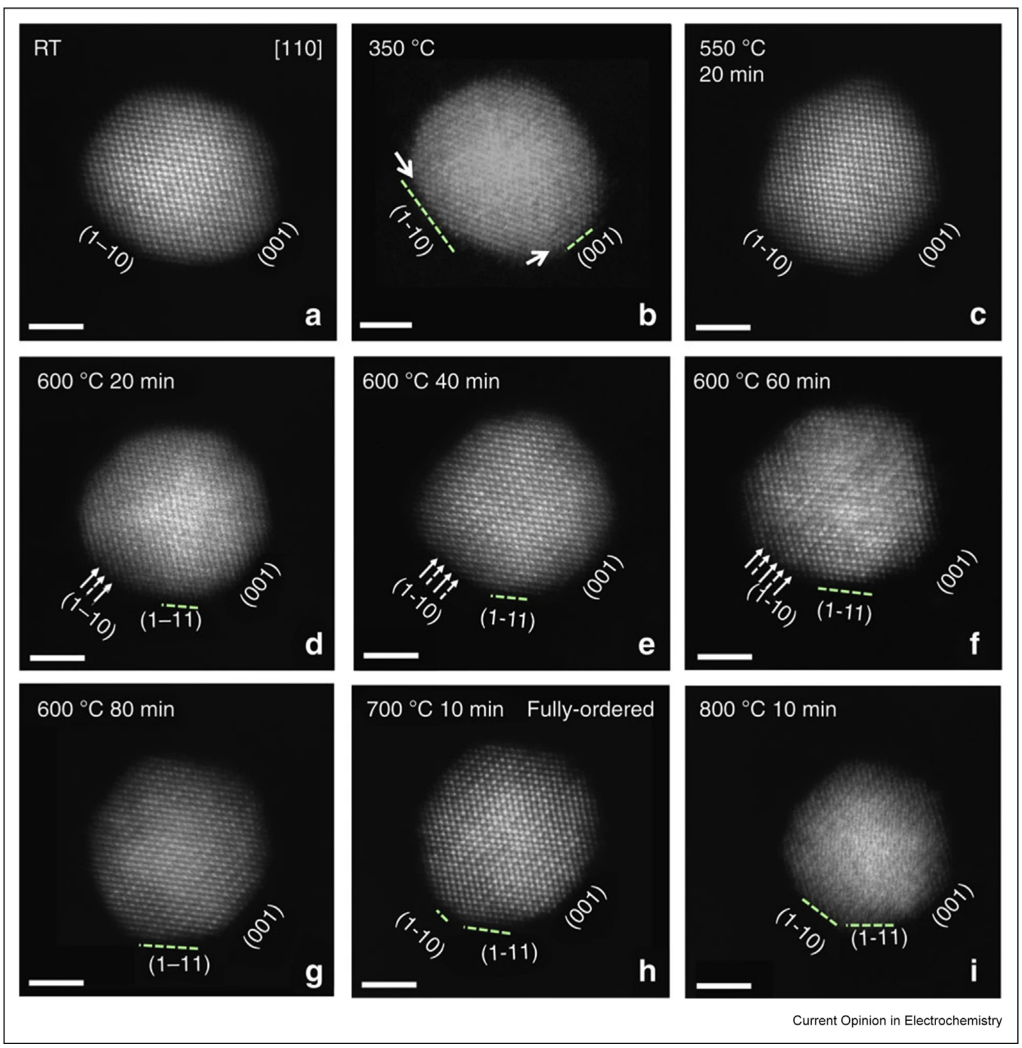

Atomic-resolution high-angle annular dark-field scanning transmission electron microscopy (HAADF-STEM) images of a Pt_3Co nanoparticle were acquired at different temperatures and annealing times. The different facets are marked on the images. The arrows in the d indicate the transition from FCC to L12 ordered phase. Adapted from the study by Chi et al. [25].

(Figure 1) [25]. In 2006, Liu et al. [24] and Strasser and Kuhl [26] described a method for producing stable Pt skins on several alloys by intentional electrochemical pre-treatment [20]. In one of these reports, it was found that dealloyed-$PtCu_3$ exhibited a ~5-fold increase in mass activity relative to Pt because of improved geometric and ligand effects provided by the core/shell structure. Stamenkovic et al. [27] found that Pt skins over Pt_3Ni (111) single crystals prepared by thermal annealing exhibited 10× enhancement for ORR relative to Pt (111) because of improved surface site availability. Snyder et al. [28] found that chemically dealloyed Pt-Ni alloys with a nanoporous morphology, with and without ionic liquid impregnation, exhibited improved mass and specific activities relative to Pt/C benchmarks.

The formation of noble metal skins on top of alloy cores is not unique to the Pt — d-block metal alloys. Several reports have found similar structures can evolve when Pt is alloyed, with f-block metals [29] and some metalloids [30,31]. The formation of noble metal shells has also been observed with alloys of Pd [32,33] and Au [34].

Morphology control of alloys formed by dealloying

Systems that form core-shell structures were found to evolve from small nanoparticles, while bicontinuous nanoporous structures with a 'spongy' morphology evolved from large nanoparticles, bulk materials, and thin films; as indicated from studies by Gan et al. [35], Gan et al. [36], McCue et al. [37], and Li et al. [38] on the Au-Ag and Pt-Ni systems, respectively [35–38]. A systematic study performed on the $PtNi_3$ system found that smaller nanoparticles formed Pt skins which protected the core and slowed down the corrosion of the non-noble metal component, whereas the larger nanoparticles lost 80% or more Ni because passivating Pt shells were not formed (Figure 2) [35,36]. Because the larger nanoparticles contained less Ni, the electronic and geometric effects were minimized, which resulted in lower intrinsic activity than nonporous particles [28].

Stability of catalysts with atomic scale ordering

Metal alloy nanocrystals can be solid solution type alloys or ordered intermetallic compounds (OIC), where the former exhibits short-range order and the latter long-range order. Reports from the early 90s have suggested that the crystal structure of an alloy can impact the stability and activity of the material. For example, an early report from Beard & Ross in 1990 found that ordered intermetallic Pt_3Co (L12 structure type) displayed higher stability than disordered alloy phases. This contrasted with reports from the study by Watanabe [17] and Yano et al. [39] in 1994 and 2017, where it was found that disordered Pt_3Co alloys exhibit higher stability (but lower activity) than ordered intermetallic Pt_3Co. This system was also examined by Wang et al. [40] in 2013, and it was found that ordered intermetallic Pt_3Co exhibited higher catalytic activity and stability for

Figure 2

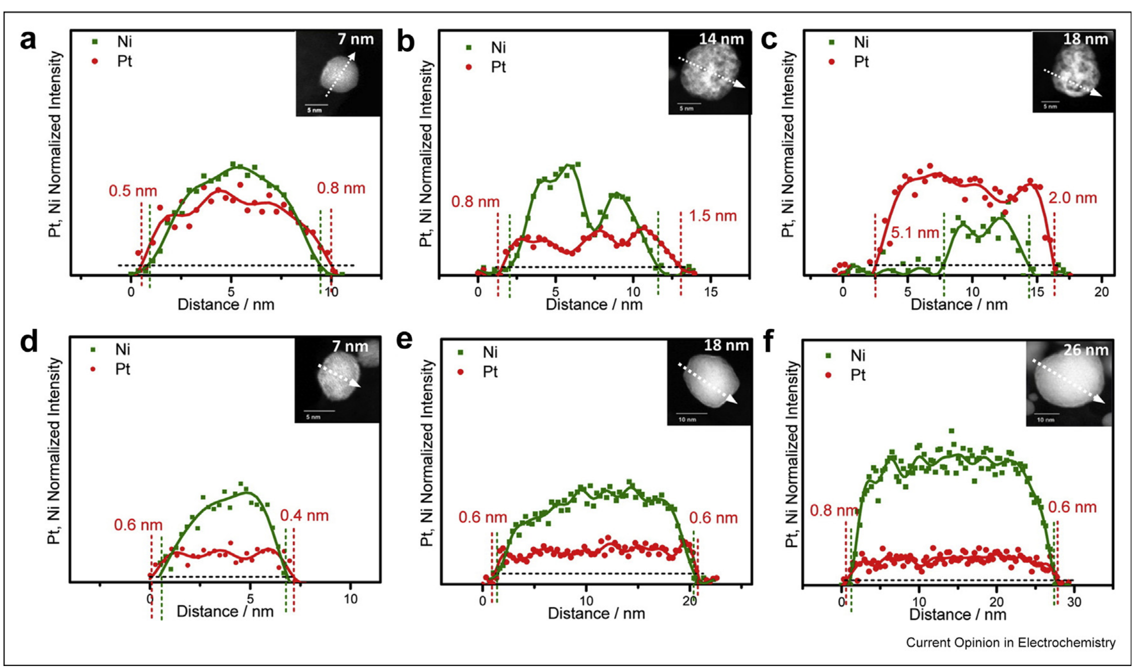

HAADF-STEM images and the corresponding electron energy loss spectroscopy line profiles of dealloyed $PtNi_3$ nanoparticles with different sizes after 10 000 cycles of stability test [35].

ORR than disordered Pt_3Co alloys. The differences in stability of ordered intermetallic Pt_3Co across the studies is related to the choice of the electrolyte, the temperature used during testing, and differences in preparation methods. Thus, it is important to consider that the stability of a catalyst can be altered by the testing conditions or preparation method. Nevertheless, most reports published in the last decade have suggested that ordered intermetallic materials exhibit higher stability and activity than disordered alloy materials with the same composition.

Ordered intermetallic compounds are expected to have a high enthalpy of mixing, contributing to improved resistance to sintering or dealloying [41]. Indeed, many ordered intermetallic phases of the Pt-X (X = Co, Ni, Fe) systems, display excellent catalytic activity relative to disordered alloy phases. For example, ordered intermetallic PtFe (L10 phase) was found to exhibit lower dissolution of Fe in comparison to disordered PtFe alloys with the same composition [42,43]. The disordered PtFe alloy had more Fe-rich clusters on the surface and sub-surface of the nanoparticles, which served as a network for Fe dissolution. The uniform mixing pattern of the ordered intermetallic phases reduced the amount of undercoordinated Fe sites near the surface, which improved the stability of the Pt skin (Figure 3).

Several other studies have shown that ordered intermetallic structures form more stable noble-metal skins than disordered alloys of the same composition, improving the stability of the system and preserving

Figure 3

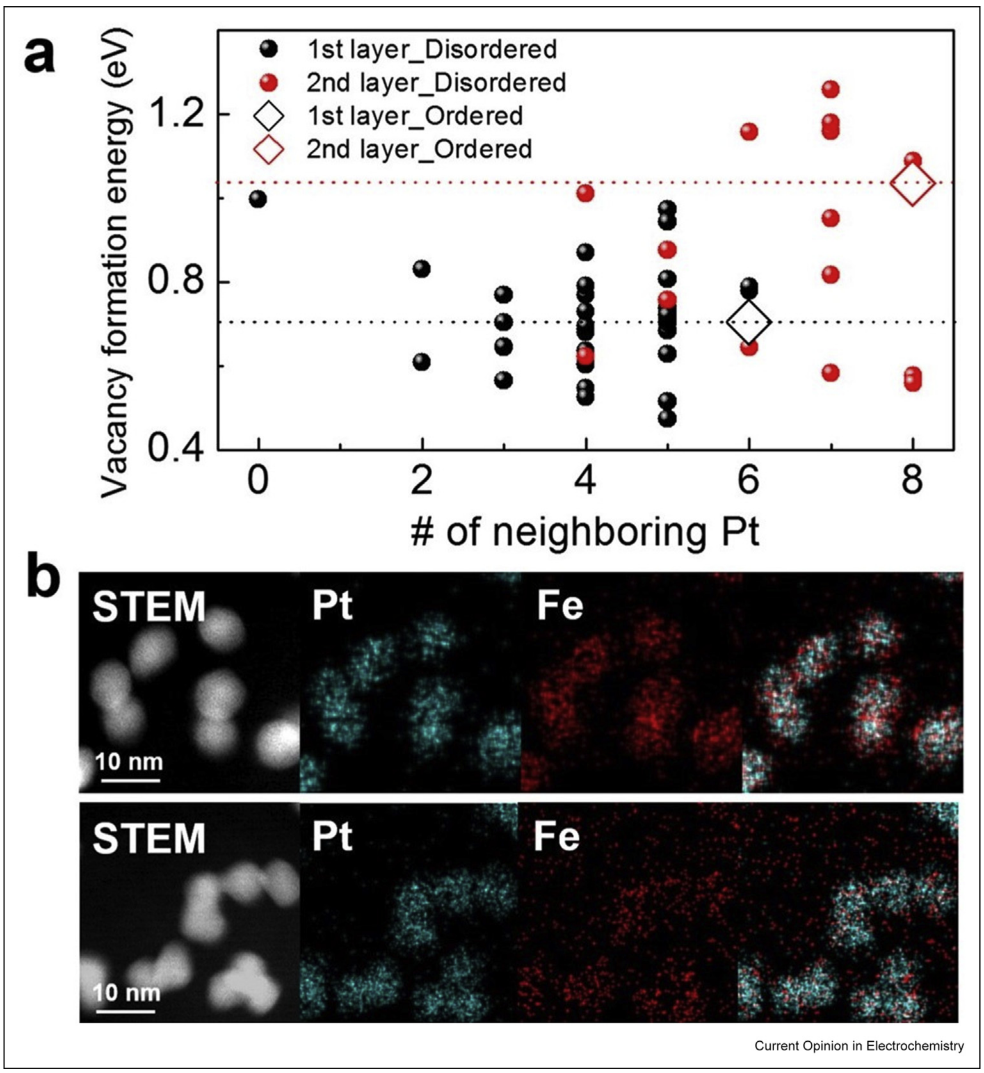

Distrubution of Fe on the surface of ordered intermetallic and disordered PtFe. (**a**) Change to the white-line intensity of the Pt L_3-edge as functions of potential measured by *in- situ* X-ray absorption near edge structure (XANES) analysis. (**b**) HAADF-STEM and energy-dispersive X-ray spectroscopy (EDS) elemental mapping analysis of ordered fct-PtFe/C (upper panel) and disordered fcc-PtFe/C (lower panel) after ADT 10000 cycles. Adapted from the study by Chung et al. [42].

high catalytic activity over long periods [30,40,42,44–46].

Doping to improve stability of alloys

Recently, it has been found that the addition of a third element to an ordered intermetallic or disordered alloy can stabilize the materials and improve the catalytic activity. The incorporation of dopants such as Au or Mo were present on the surface of the alloy and passivated dissolution sites, leading to increased stability [45,47,48]. For example, incorporation of Au into the Pd_6CoCu system led to a partial replacement of Co and Cu on the surface and within the bulk of the material, improving stability (Figure 4) [42]. Doping ordered intermetallic Pd–Zn alloys with Au reduced the dissolution of Zn, limiting the Pd skin thickness to < 1 nm [33]. In contrast, Pd-Zn alloys without Au incorporation formed 3 nm Pd shells [33]. Huang et al. [49] found that doping Pt_3Ni alloys with Mo improved the activity and stability of ORR. The surface doped Pt_3Ni displayed a ∼6% decrease of specific activity after 8000 cycles, while undoped Pt_3Ni decreased by 67% from large compositional and morphological changes. DFT calculations suggested that the Mo atoms occupy the edge or vertex site inhibiting surface diffusion and stabilizing the surface Pt and Ni atoms [50].

Mechanisms of dealloying

As mentioned in the preceding sections, conventional wisdom has indicated that alloy nanomaterials can evolve to the following (1) core-–shell particles, or (2) bi-continuous nanoporous metals. When a binary alloy consisting of a noble metal and non-noble metal is placed in solution under oxidizing conditions, the non-

Figure 4

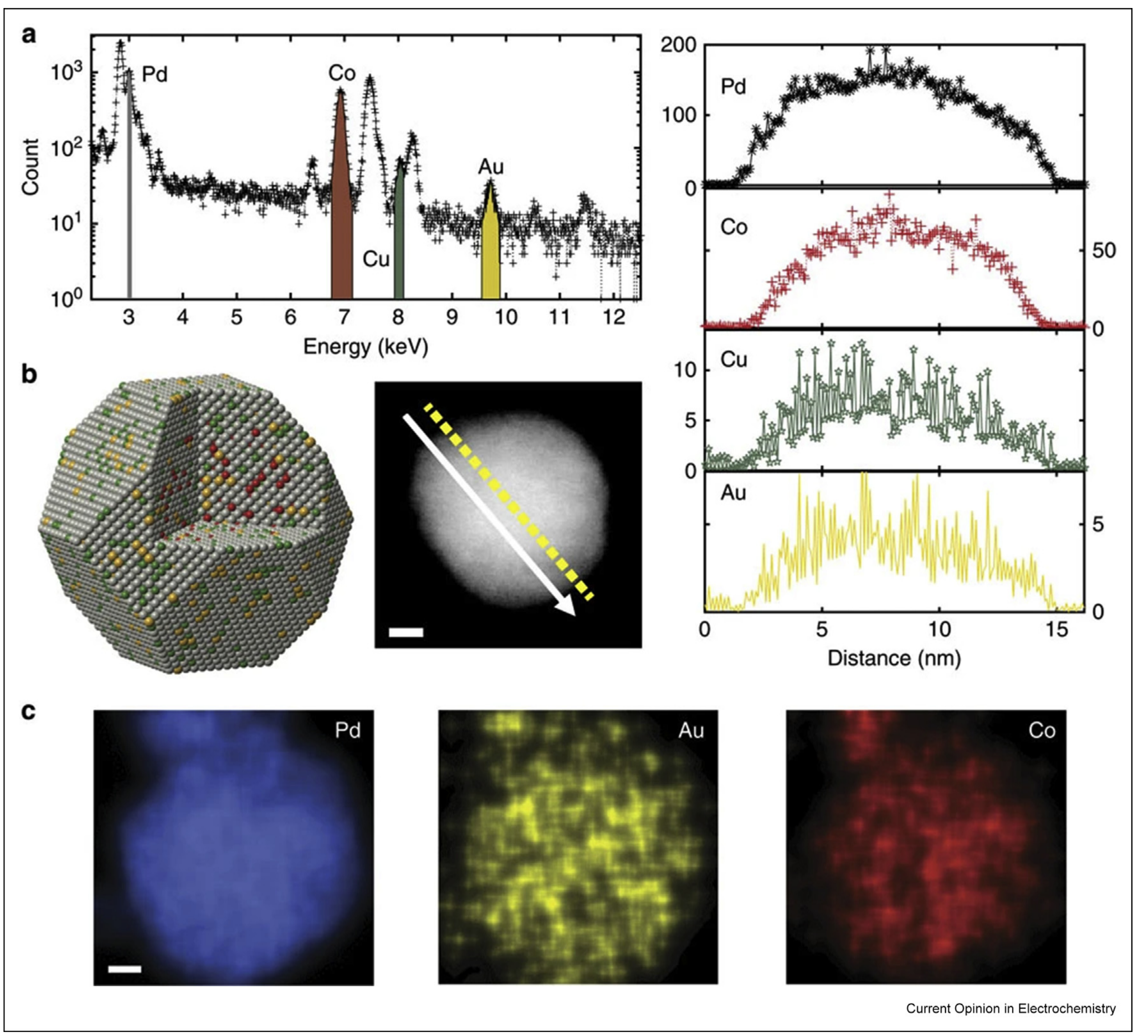

The composition analysis showing the uniformity of the elements of Au-Pd_6CoCu/C nanoparticles. (**a**) Energy-dispersive X-ray spectroscopic (EDX) analysis of the nanoparticle. (**b**) Elemental distribution of Pd, Co, Cu, and Au in a single Au-Pd_6CoCu/C nanoparticle extracted from an aberration-corrected scanning transmission electron microscopy energy-dispersive X-ray spectroscopy (STEM-EDX) line profile. Scale bar, 2 nm. (**c**) Aberration-corrected STEM-EDX 2D elemental maps of Pd, Co, and Au. Scale bar, 5 nm. Adapted from the study by Wang et al. [51].

noble metal component can be removed when the voltage is above its corrosion potential, enriching the material with noble metal in a process known as dealloying. The evolution of porosity or formation of shells depends on the interplay between the diffusion of the noble metal atoms on the surface and the dissolution rate of the non-noble metal component (Figure 5). The enrichment and surface diffusion of the noble metal cause clusters to form on the surface of the material; these clusters grow as the non-noble metal is continuously removed. If there is not enough noble metal to fully passivate the surface, that is, form a Pt skin or thin shell, then the less noble metal will continue to dissolve causing nanoporosity to occur. The rate of surface diffusivity is linked to the ligament size that will form during dealloying. Systematic studies by Snyder et al. [28], McCue et al. [37], and Li et al. [38] have shown that ligament size

Figure 5

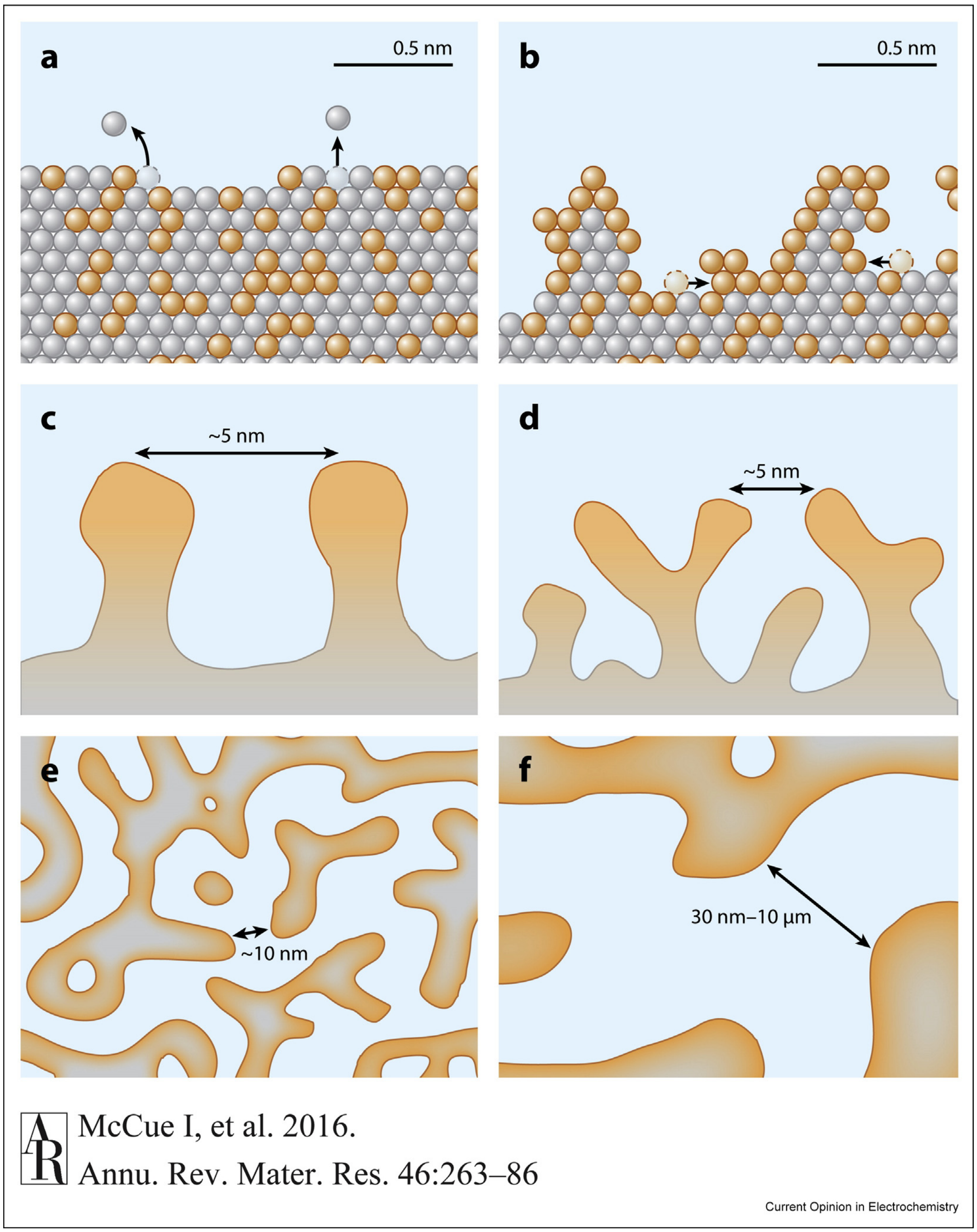

Schematic depicting the (**a**) dissolution of Ag from Au-Ag alloys, (**b**) enrichment of surface with Au adatoms, surface diffusion of Au, and island formation, and (**c**), **(d), (e),** and (**f**) Evolution of ligament formation, and ligament coarsening. Adapted from the study by McCue et al. [37].

of dealloyed Ni-Pt and Ag-Au was 2 nm and 4 nm, respectively. Nanoparticles with diameters less than the ligament size were unable to form bi-continuous nanoporous structures and instead formed core-shell structures.

In contrast, nanoparticles and other morphologies (thin films, bulk materials, and so on) with feature size greater than the ligament size can form bi-continuous nanoporous structures. The mechanisms of pore formation in dealloyed materials have been discussed in several other manuscripts [52–54] and reviews [37,55], which the reader is referred to for more comprehensive information.

Evolution of crystal structure during corrosive electrocatalytic conditions

The crystal structure of alloys can be altered during catalysis. For solid solution type alloys with wide solubility ranges, for example, Au-Ag, changes to the composition of the material as Ag is removed would not lead to changes in the crystal structure. However, some OICs can only permit limited changes to the composition before the crystal structure will change, as indicated by thermodynamic stability from the phase diagram. When the deviations of the composition exceed what is thermodynamically allowed, then the OIC can restructure into another phase to reduce its Gibbs free energy. This is usually achieved by the disordering of the lattice or by transforming the OIC to a disordered solid solution alloy. For example, corrosion-based disordering has been observed on ordered intermetallic Pt_3Co when the composition of the material deviates from the stability range of the OIC phase [17].

Electrochemically induced incongruent phase transformations

Recently, Sun et al. [56] has reported a new pathway for the structural evolution of alloys during electrochemical catalysis. In this report, it was found that ordered intermetallic $PdBi_2$ (I4/mmm space group) transformed to Pd_3Bi (Pmma space group) by potential cycling under ORR conditions or inert gas (Figure 6). This result was striking because it demonstrated that an OIC can transform into another OIC with different composition and crystal structure under ambient temperature and pressure.

It was found that the formation of crystalline Pd shells over Pd_3Bi cores (orthorhombic lattice) is kinetically hindered as the crystal structure and lattice constants vary considerably from the ground state of elemental Pd (FCC). After 10,000 cycles, the phase converted Pd_3Bi maintained crystallinity even though ~3% of the Bi was lost from the material. Pd_3Bi prepared by the electrochemically driven incongruent phase transformation exhibited an 11× improvement relative to Pt/C catalysts, which is among the highest mass and specific activities measured for a Pd-based material for ORR [57]. High-performance ORR activity was also found for $Pd_{31}Bi_{12}$, a metastable phase similar in composition to Pd_3Bi [58,59].

Factors which control the dealloying pathway of alloy nanomaterials

Metal alloys can undergo several types of structural transformations during corrosion by forming core-shell nanoparticles, bicontinuous nanoporous metals, or conversion to an intermetallic phase with a different composition and crystal structure than the starting material.

Figure 6

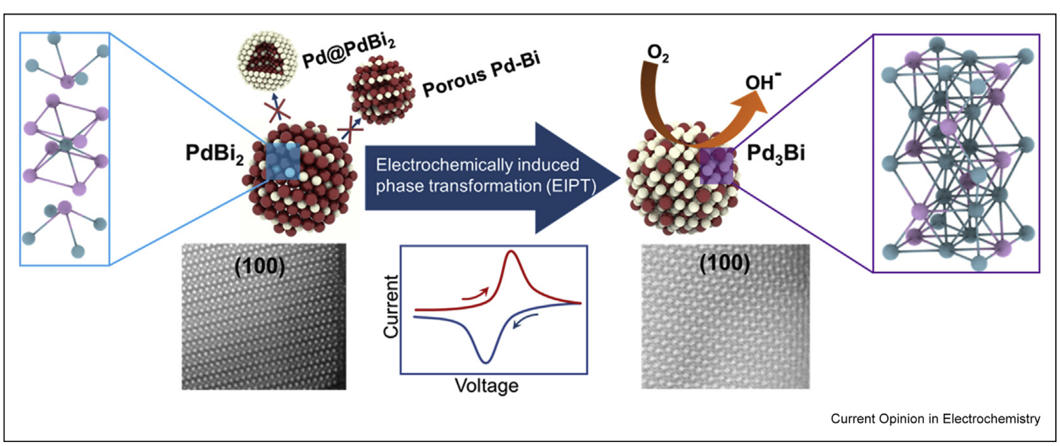

Schematic, TEM image, and cyclic voltammogram depicting the conversion of ordered intermetallic $PdBi_2$ to ordered intermetallic Pd_3Bi through an electrochemically driven incongruent phase transformation at room temperature. Adapted from the study by Sun et al. [56]. TEM, transmission electron microscopy.

To understand which pathway a material will undergo, it is important to carefully consider the properties of the initial starting material. There are two points that must be carefully considered: (1) the thermodynamic stability of phases, (2) the kinetics of diffusion within the bulk and surface.

First, bulk phase diagrams need to be assessed; if intermetallic phases are not present on the phase diagram, then conversion to intermetallic phases is unlikely. Next, it is important to consider the thermodynamic stability of a material in an aqueous electrolyte as a function of potential and pH (Pourbaix diagrams). Multiple ordered intermetallic phases, such as Pd_3Bi, PdBi, and Pd_5Bi_2, and elemental Pd, are observed from the oxidative dissolution of Bi from $PdBi_2$, with the stability range of each phase depending on the applied voltage (Figure 7).

Kinetic factors must also be considered because interdiffusion within the bulk of the material is necessary for crystal lattice reorganization to take place. We investigated the rate of the phase conversion of $PdBi_2$ to Pd_3Bi to shed light on the importance of fast diffusivity [56]. We used density functional theory [60] to calculate the minimum diffusion activation energy of Bi atoms in $PdBi_2$, assuming a vacancy-mediated diffusion mechanism. The lowest activation barrier for Bi diffusion in $PdBi_2$ is 42 kJ/mol (0.44 eV), corresponding to a two-dimensional migration pathway. We found that diffusion of Bi through $PdBi_2$ is likely facilitated by high vacancy concentrations because the calculated vacancy formation energy for Bi along the diffusion path is only 0.17 eV relative to bulk Bi. We estimated that at room temperature, the root mean square displacement of Bi in $PdBi_2$ reaches a typical particle width (~20 nm) in well less than 1 s. This result indicated that Bi diffusion in $PdBi_2$ is facile, enabling the rapid removal of Bi from the material. The low melting point of $PdBi_2$ suggests that it has low vacancy formation energies, which facilitates the removal of the Bi from the surface and promotes interdiffusion of the constituent atoms [61,62].

The low melting point of the starting material is an important indicator for bulk restructuring to occur since the atoms with high atomic diffusivity can reorganize into another state. In contrast, materials with high melting points (e.g. Pt-Co, Pt-Ni, Pt-Fe, and so on) cannot undergo conversion to another OIC phase since bulk diffusion is too low. It is possible that other low melting point OIC materials besides the Pd-Bi system can undergo lattice reorganization during dealloying; this is currently an ongoing effort of exploration in the Hall laboratory.

Future outlook

This review covers recent progress on the preparation and stability of alloy nanoparticles under electrochemical conditions. During electrochemical catalysis, the non-noble element can corrode, resulting in structural and morphological changes to the catalyst. The formation of core-shell structures or bi-continuous nanoporous materials is commonly observed. However, it was recently found by Sun et al. [56] that low-

Figure 7

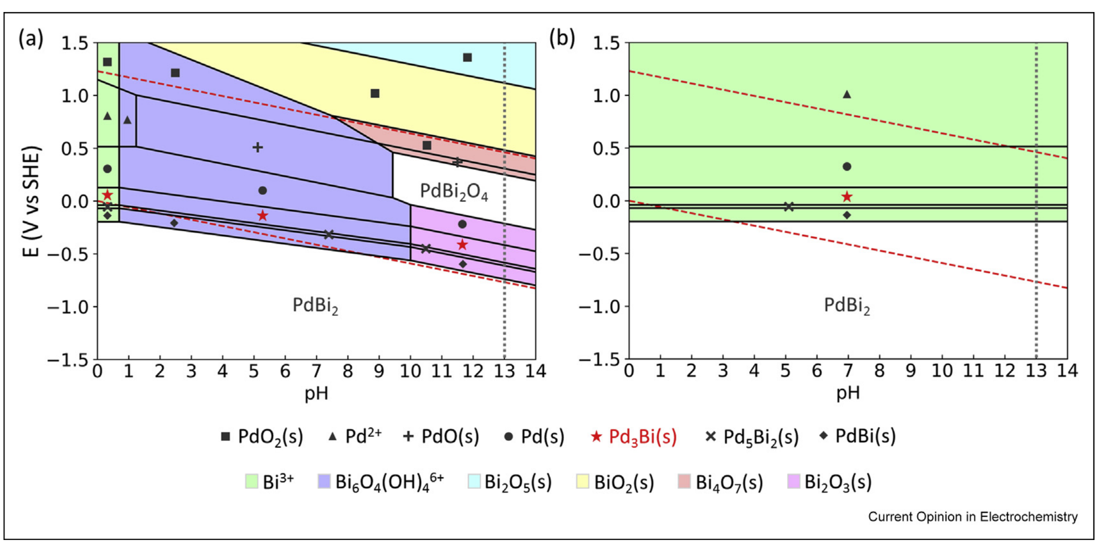

Electrochemical stability of $PdBi_2$. (**a**) The calculated Pourbaix diagram (**b**) and modified Pourbaix diagram excluding the oxide. The dashed lines indicate the electrochemical stability window for water, with the lower line corresponding to the RHE and the upper line corresponding to the thermodynamic potential for the H_2O/O_2. Adapted from the study by Sun et al. [56]. RHE, reversible hydrogen electrode.

melting–point OICs can undergo bulk reconstructions to another OIC with a different composition and crystal structure in voltage ranges relevant to electrochemical catalysis. It is important for researchers to carefully evaluate the crystal structure and composition of catalysts after stability testing to identify if electrochemically induced phase transformations have occurred; particularly if intermetallic materials with low melting points are being used as the catalyst. While electrochemically induced-phase transformations were originally used as a synthetic tool for preparing OICs at room temperature, this knowledge can be used to understand the stability of materials under electrocatalytic conditions.

Declaration of competing interest

The authors declare that they have no known competing financial interests or personal relationships that could have appeared to influence the work reported in this paper.

Acknowledgements

A.S.H. acknowledges financial support from the National Science Foundation under award no. CHE-1764310, DMR-2047019, the Johns Hopkins Catalyst Award, and the Sloan Foundation.

References

Papers of particular interest, published within the period of review, have been highlighted as:

* of special interest
** of outstanding interest

1. Cano ZP, Banham D, Ye SY, Hintennach A, Lu J, Fowler M, Chen ZW: **Batteries and fuel cells for emerging electric vehicle markets**. *Nat Energy* 2018, **3**:279–289.

2. * Tong WM, Forster M, Dionigi F, Dresp S, Erami RS, Strasser P, Cowan AJ, Farras P: **Electrolysis of low-grade and saline surface water**. *Nat Energy* 2020, **5**:367–377.
The authors reviewed the opportunities and challenges of electrolysis of saline water, where the performance and stability will be influenced by prevelant chloride ions.

3. Schmidt O, Hawkes A, Gambhir A, Staffell I: **The future cost of electrical energy storage based on experience rates**. *Nat Energy* 2017, **2**:17110.

4. Mohle S, Zirbes M, Rodrigo E, Gieshoff T, Wiebe A, Waldvogel SR: **Modern electrochemical aspects for the synthesis of value-added organic products**. *Angew Chem Int Ed Engl* 2018, **57**:6018–6041.

5. De Luna P, Hahn C, Higgins D, Jaffer SA, Jaramillo TF, Sargent EH: **What would it take for renewably powered electrosynthesis to displace petrochemical processes?** *Science* 2019, **364**. eaav3506.

6. Seh ZW, Kibsgaard J, Dickens CF, Chorkendorff I, Norskov JK, Jaramillo TF: **Combining theory and experiment in electrocatalysis: insights into materials design**. *Science* 2017, **355**, eaad4998.

7. Bing Y, Liu H, Zhang L, Ghosh D, Zhang J: **Nanostructured pt-alloy electrocatalysts for pem fuel cell oxygen reduction reaction**. *Chem Soc Rev* 2010, **39**:2184–2202.

8. Pivovar B: **Catalysts for fuel cell transportation and hydrogen related uses**. *Nat Catal* 2019, **2**:562–565.

9. Hu JW, Sui PC, Kumar S, Djilali N: **Modelling and simulations of carbon corrosion during operation of a polymer electrolyte membrane fuel cell**. *Electrochim Acta* 2009, **54**:5583–5592.

10. Jia QY, Ramaker DE, Ziegelbauer JM, Ramaswamy N, Halder A, Mukerjee S: **Fundamental aspects of ad-metal dissolution and contamination in low and medium temperature fuel cell electrocatalysis: a cu based case study using in situ electrochemical x-ray absorption spectroscopy**. *J Phys Chem C* 2013, **117**:4585–4596.

11. Inventor Noble metal-refractory metal alloys as catalysts and method for making. Patent 1980.

12. Inventor Noble metal/vanadium alloy catalyst and method for making. Patent 1980.

13. Inventor Noble metal-chromium alloy catalysts and electrochemical cell. Patent 1982.

14. Inventor Ternary fuel cell catalysts containing platinum, cobalt and chromium. Patent 1984.

15. Inventor Ordered ternary fuel cell catalysts containing platinum and cobalt and method for making the catalysts. Patent 1987.

16. Beard BC: **The structure and activity of pt-co alloys as oxygen reduction electrocatalysts**. *J Electrochem Soc* 1990, **137**:3368.

17. Watanabe M: **Activity and stability of ordered and disordered co-pt alloys for phosphoric acid fuel cells**. *J Electrochem Soc* 1994, **141**:2659.

18. Toda T: **Enhancement of the electroreduction of oxygen on pt alloys with fe, ni, and co**. *J Electrochem Soc* 1999, **146**:3750.

19. Rudi S, Teschner D, Beermann V, Hetaba W, Gan L, Cui C, Gliech M, Schlögl R, Strasser P: **Ph-induced versus oxygen-induced surface enrichment and segregation effects in Pt–Ni alloy nanoparticle fuel cell catalysts**. *ACS Catal* 2017, **7**:6376–6384.

20. Inventor Corrosion and ORR activity of pt alloy electrocatalysts during voltammetric pretreatment. Patent 2006.

21. * Wang C, Chi M, Li D, Strmcnik D, van der Vliet D, Wang G, Komanicky V, Chang K-C, Paulikas AP, Tripkovic D, Pearson J, More KL, Markovic NM, Stamenkovic VR: **Design and synthesis of bimetallic electrocatalyst with multilayered pt-skin surfaces**. *J Am Chem Soc* 2011, **133**:14396–14403.
This paper descibe a method of pretreating PtNi nanoparticles to create stable Pt-shells for ORR.

22. Wang C, Wang G, van der Vliet D, Chang K-C, Markovic NM, Stamenkovic VR: **Monodisperse Pt3co nanoparticles as electrocatalyst: the effects of particle size and pretreatment on electrocatalytic reduction of oxygen**. *Phys Chem Chem Phys* 2010, **12**:6933–6939.

23. Mani P, Srivastava R, Strasser P: **Dealloyed pt–cu core–shell nanoparticle electrocatalysts for use in pem fuel cell cathodes**. *J Phys Chem C* 2008, **112**:2770–2778.

24. Liu ZC, Koh S, Yu CF, Strasser P: **Synthesis, dealloying, and orr electrocatalysis of pdda-stabilized cu-rich pt alloy nanoparticles**. *J Electrochem Soc* 2007, **154**:B1192–B1199.

25. Chi M, Wang C, Lei Y, Wang G, Li D, More KL, Lupini A, Allard LF, Markovic NM, Stamenkovic VR: **Surface faceting and elemental diffusion behaviour at atomic scale for alloy nanoparticles during in situ annealing**. *Nat Commun* 2015, **6**:8925.

26. Strasser P, Kuhl S: **Dealloyed pt-based core-shell oxygen reduction electrocatalysts**. *Nanomater Energy* 2016, **29**:166–177.

27. Stamenkovic VR, Fowler B, Mun BS, Wang G, Ross PN, Lucas CA, Marković NM: **Improved oxygen reduction activity on $Pt_3Ni(111)$ via increased surface site availability**. *Science* 2007, **315**:493–497.

28. Snyder J, Fujita T, Chen MW, Erlebacher J: **Oxygen reduction in nanoporous metal–ionic liquid composite electrocatalysts**. *Nat Mater* 2010, **9**:904–907.

29. Escudero-Escribano M, Malacrida P, Hansen MH, Vej-Hansen UG, Velazquez-Palenzuela A, Tripkovic V, Schiotz J, Rossmeisl J, Stephens IE, Chorkendorff I: **Tuning the activity of**

pt alloy electrocatalysts by means of the lanthanide contraction. *Science* 2016, **352**:73–76.

30. Bu L, Zhang N, Guo S, Zhang X, Li J, Yao J, Wu T, Lu G, Ma JY, Su D, Huang X: **Biaxially strained ptpb/pt core/shell nanoplate boosts oxygen reduction catalysis**. *Science* 2016, **354**: 1410–1414.

31. Qin Y, Luo M, Sun Y, Li C, Huang B, Yang Y, Li Y, Wang L, Guo S: **Intermetallic hcp-ptbi/fcc-pt core/shell nanoplates enable efficient bifunctional oxygen reduction and methanol oxidation electrocatalysis**. *ACS Catal* 2018, **8**:5581–5590.

32. Gunji T, Noh SH, Tanabe T, Han B, Nien CY, Ohsaka T, Matsumoto F: **Enhanced electrocatalytic activity of carbon-supported ordered intermetallic palladium–lead (pd3pb) nanoparticles toward electrooxidation of formic acid**. *Chem Mater* 2017, **29**:2906–2913.

33. ** Yang Y, Xiao W, Feng X, Xiong Y, Gong M, Shen T, Lu Y, Abruña HD, Wang D: **Golden palladium zinc ordered intermetallics as oxygen reduction electrocatalysts**. *ACS Nano* 2019, **13**:5968–5974.

The authors exhibit the state-of-art method for doping Au into nanomaterials to enhance its stability. Interestingly, the Au does not only stabilize the surface but also penetrates into the crystal lattice.

34. Sun K, Cheng T, Wu L, Hu Y, Zhou J, Maclennan A, Jiang Z, Gao Y, Goddard WA, Wang Z: **Ultrahigh mass activity for carbon dioxide reduction enabled by gold–iron core–shell nanoparticles**. *J Am Chem Soc* 2017, **139**:15608–15611.

35. Gan L, Heggen M, O'Malley R, Theobald B, Strasser P: **Understanding and controlling nanoporosity formation for improving the stability of bimetallic fuel cell catalysts**. *Nano Lett* 2013, **13**:1131–1138.

36. Gan L, Cui C, Rudi S, Strasser P: **Core–shell and nanoporous particle architectures and their effect on the activity and stability of pt orr electrocatalysts**. *Top Catal* 2013, **57**: 236–244.

37. * McCue I, Benn E, Gaskey B, Erlebacher J: **Dealloying and dealloyed materials**. *Annu Rev Mater Res* 2016, **46**:263–286.

This paper provides a comprehensive review on the mechanisms of the microstructural evolution of dealloyed materials.

38. Li X, Chen Q, McCue I, Snyder J, Crozier P, Erlebacher J, Sieradzki K: **Dealloying of noble-metal alloy nanoparticles**. *Nano Lett* 2014, **14**:2569–2577.

39. Yano H, Arima I, Watanabe M, Iiyama A, Uchida H: **Oxygen reduction activity and durability of ordered and disordered pt3co alloy nanoparticle catalysts at practical temperatures of polymer electrolyte fuel cells**. *J Electrochem Soc* 2017, **164**: F966–F972.

40. Wang D, Xin HL, Hovden R, Wang H, Yu Y, Muller DA, DiSalvo FJ, Abruna HD: **Structurally ordered intermetallic platinum-cobalt core-shell nanoparticles with enhanced activity and stability as oxygen reduction electrocatalysts**. *Nat Mater* 2013, **12**:81–87.

41. Antolini E: **Alloy vs. Intermetallic compounds: effect of the ordering on the electrocatalytic activity for oxygen reduction and the stability of low temperature fuel cell catalysts**. *Appl Catal, B* 2017, **217**:201–213.

42. Chung DY, Jun SW, Yoon G, Kwon SG, Shin DY, Seo P, Yoo JM, Shin H, Chung YH, Kim H, Mun BS, Lee KS, Lee NS, Yoo SJ, Lim DH, Kang K, Sung YE, Hyeon T: **Highly durable and active ptfe nanocatalyst for electrochemical oxygen reduction reaction**. *J Am Chem Soc* 2015, **137**:15478–15485.

43. Kim J, Lee Y, Sun S: **Structurally ordered FePt nanoparticles and their enhanced catalysis for oxygen reduction reaction**. *J Am Chem Soc* 2010, **132**:4996–4997.

44. ** Cao L, Zhao ZP, Liu ZY, Gao WP, Dai S, Gha J, Xue W, Sun HT, Duan XF, Pan XQ, Mueller T, Huang Y: **Differential surface elemental distribution leads to significantly enhanced stability of PtNi-based orr catalysts**. *Matter* 2019, **1**:1567–1580.

The authors combines experimental and computational methods to reveal how the elemental distribution of atoms on the surface control PtNi corrosion during ORR. It highlights the importance of the elemental distribtion of atoms on the surface for improving long term stability.

45. Wang D, Liu S, Wang J, Lin R, Kawasaki M, Rus E, Silberstein KE, Lowe MA, Lin F, Nordlund D, Liu H, Muller DA, Xin HL, Abruna HD: **Spontaneous incorporation of gold in palladium-based ternary nanoparticles makes durable electrocatalysts for oxygen reduction reaction**. *Nat Commun* 2016, **7**:11941.

46. Cui Z, Chen H, Zhao M, DiSalvo FJ: **High-performance Pd3Pb intermetallic catalyst for electrochemical oxygen reduction**. *Nano Lett* 2016, **16**:2560–2566.

47. Pizzutilo E, Freakley SJ, Geiger S, Baldizzone C, Mingers A, Hutchings GJ, Mayrhofer KJJ, Cherevko S: **Addressing stability challenges of using bimetallic electrocatalysts: the case of gold–palladium nanoalloys**. *Catal Sci Technol* 2017, **7**: 1848–1856.

48. Kuttiyiel KA, Sasaki K, Su D, Wu L, Zhu Y, Adzic RR: **Gold-promoted structurally ordered intermetallic palladium cobalt nanoparticles for the oxygen reduction reaction**. *Nat Commun* 2014, **5**:5185.

49. Huang X, Zhao Z, Cao L, Chen Y, Zhu E, Lin Z, Li M, Yan A, Zettl A, Wang YM, Duan X, Mueller T, Huang Y: **Electrochemistry. High-performance transition metal-doped Pt_3Ni octahedra for oxygen reduction reaction**. *Science* 2015, **348**:1230–1234.

50. Cao L, Mueller T: **Theoretical insights into the effects of oxidation and mo-doping on the structure and stability of Pt–Ni nanoparticles**. *Nano Lett* 2016, **16**:7748–7754.

51. Wang D, Liu S, Wang J, Lin R, Kawasaki M, Rus E, Silberstein KE, Lowe MA, Lin F, Nordlund D, Liu H, Muller DA, Xin HL, Abruna HD: **Spontaneous incorporation of gold in palladium-based ternary nanoparticles makes durable electrocatalysts for oxygen reduction reaction**. *Nat Commun* 2016, **7**:11941.

52. * Liu P, Chen Q, Ito Y, Han J, Chu S, Wang X, Reddy KM, Song S, Hirata A, Chen M: **Dealloying kinetics of AgAu nanoparticles by in situ liquid-cell scanning transmission electron microscopy**. *Nano Lett* 2020, **20**:1944–1951.

This is the latest observation for the AgAu model of dealloying kinetics. The particle-size-dependent dealloying behavior is viewed in realtime by in-situ TEM.

53. Mccue I, Gaskey B, Geslin PA, Karma A, Erlebacher J: **Kinetics and morphological evolution of liquid metal dealloying**. *Acta Mater* 2016, **115**:10–23.

54. Wang Z, Liu P, Han J, Cheng C, Ning S, Hirata A, Fujita T, Chen M: **Engineering the internal surfaces of three-dimensional nanoporous catalysts by surfactant-modified dealloying**. *Nat Commun* 2017, **8**:1066.

55. Chen Q, Ding Y, Chen MW: **Nanoporous metal by dealloying for electrochemical energy conversion and storage**. *MRS Bull* 2018, **43**:43–48.

56. ** Sun D, Wang Y, Livi KJT, Wang C, Luo R, Zhang Z, Alghamdi H, Li C, An F, Gaskey B, Mueller T, Hall AS: **Ordered intermetallic Pd_3Bi prepared by an electrochemically induced phase transformation for oxygen reduction electrocatalysis**. *ACS Nano* 2019, **13**:10818–10825.

The authors revealed the structural elvolution of Pd-Bi alloys during electrochemical operation. It is the first report of the conversion of one ordered intermetallic material into another ordered intermetallic material with a different crystal structure and composition at room temperature.

57. Wang Y, Sun D, Wang M, Feng Z, Hall AS: **Oxygen reduction electrocatalysis on ordered intermetallic Pd-Bi electrodes is enhanced by low coverage of spectator species**. *J Phys Chem C* 2020, **124**:5220–5224.

58. Wang Y, Sun D, Chowdhury T, Wagner JS, Kempa TJ, Hall AS: **Rapid room-temperature synthesis of a metastable ordered intermetallic electrocatalyst**. *J Am Chem Soc* 2019, **141**: 2342–2347.

59. Wang Y, Hall AS: **Pulsed electrodeposition of metastable $Pd_{31}Bi_{12}$ nanoparticles for oxygen reduction electrocatalysis**. *ACS Energy Lett* 2019:17–22.

60. Kohn W, Sham LJ: **Self-consistent equations including exchange and correlation effects**. *Phys Rev* 1965, **140**: A1133–A1138.

61. Medasani B, Haranczyk M, Canning A, Asta M: **Vacancy formation energies in metals: a comparison of metagga with lda and gga exchange–correlation functionals**. *Comput Mater Sci* 2015, **101**:96–107.

62. Otake S, Ishii Y, Matsuno N: **Migration energy of vacancies in bismuth**. *Jpn J Appl Phys* 1981, **20**:1037–1040.